J. Fluid Mech. (1989), *vol.* 207, *pp.* 97–120
Printed in Great Britain

Nonlinear evolution of interacting oblique waves on two-dimensional shear layers

By M. E. GOLDSTEIN AND S.-W. CHOI
National Aeronautics and Space Administration, Lewis Research Center, Cleveland, OH 44135, USA

(Received 27 October 1988)

We consider the effects of critical-layer nonlinearity on spatially growing oblique instability waves on nominally two-dimensional shear layers between parallel streams. The analysis shows that three-dimensional effects cause nonlinearity to occur at much smaller amplitudes than it does in two-dimensional flows. The nonlinear instability wave amplitude is determined by an integro–differential equation with cubic-type nonlinearity. The numerical solutions to this equation are worked out and discussed in some detail. We show that they always end in a singularity at a finite downstream distance.

1. Introduction

External excitation of (convectively unstable) free shear layers between parallel streams produces spatially growing instability waves that are initially governed by linear dynamics for sufficiently small excitation amplitudes. While the instability amplitude continues to increase with increasing downstream distance, its local growth rate must ultimately decrease due to viscous spreading of the mean shear layer. Nonlinear effects can then become important in a 'critical layer' at the transverse position where the mean flow and instability wave phase velocities are equal (once the instability wave amplitude becomes sufficiently large and its growth rate becomes sufficiently small). The unsteady critical-layer flow is then governed by a nonlinear vorticity equation, while the motion outside the critical layer remains essentially linear. The external instability wave growth rate is, however, completely controlled by the nonlinear dynamics of the critical layer.

There are now too many nonlinear critical layer analyses in the literature for us to summarize here. We refer the reader to the excellent review by Maslowe (1986) for nonlinear critical layers in general and to the one by Stewartson (1981) for Rossby-wave critical layers in particular. Here it is only appropriate to mention the analyses specifically concerned with spatially evolving flows. Huerre (1980, 1987) considers the two-dimensional incompressible shear layer in the viscous critical-layer regime where the nonlinear effects enter only at higher order. Huerre & Scott (1980) and Robinson (1974) consider the strongly nonlinear regime, but their choice of scaling precludes the possibility of matching their results onto the linear upstream solution.

Goldstein & Leib (1988) and Goldstein & Hultgren (1988) overcame this difficulty, but again consider only the incompressible case. They consider only a two-dimensional flow, since the two-dimensional instability wave is the most rapidly growing linear mode in that case. However, oblique modes exhibit the most rapid growth in sufficiently high-Mach-number supersonic shear layers (Gropengeisser 1969; Jackson & Grosch 1988). Goldstein & Leib (1989) consider the case where the

unsteady flow evolves from a single oblique mode, in which case it is appropriate to suppose that the initial instability wave grows in its propagation direction. The cross-flow velocity effects can then be eliminated from the analysis by use of an appropriate 'Squire transform', but the critical-layer nonlinearity still behaves quite differently from the incompressible case – primarily because the temperature fluctuations have algebraic singularities in the critical layer and therefore become very large relative to the velocity components, causing the critical-layer nonlinearity to occur at a much smaller amplitude *vis-à-vis* the two-dimensional isothermal case. The resulting critical-layer nonlinearity is then weak in the sense that the flow is governed by linear dynamics to lowest order of approximation, with nonlinearity entering only through the higher-order (inhomogeneous) terms. The instability wave growth rate is still controlled by the nonlinear terms, but can now be calculated from an amplitude equation similar to the one found by Hickernell (1984) for the Rossby-wave singular modes.

Here, we consider the case where the initial instability wave grows in the streamwise direction. It is then appropriate to suppose that there are two oblique modes with the same frequency and streamwise wavenumber but with equal and opposite (real) spanwise wavenumbers in order to represent a fixed spanwise structure. (In real flows the allowable spanwise wavenumbers might be selected by the sidewall positions.) The cross-flow velocity fluctuations, which have the same algebraic singularity in the critical layer as the temperature fluctuations, now become coupled to the velocity fluctuations in the plane of the wave, causing the critical-layer nonlinearity to again become important at smaller amplitudes than in the two-dimensional incompressible case. In fact, the nonlinear oblique-mode interaction causes the critical-layer nonlinearity to occur at even smaller amplitudes than in the single-mode compressible case (Goldstein & Leib 1989). Critical-layer nonlinearity now becomes important when the instability wave growth rate is $O(\epsilon^{\frac{1}{5}})$ rather than $O(\epsilon^{\frac{2}{5}})$, as in the Goldstein & Leib (1989) case, where ϵ denotes the characteristic instability wave amplitude at the start of the nonlinear region.

The instability amplitude outside the critical layer can again be determined from an amplitude equation because the critical-layer nonlinearity is still weak. The equation is similar to that of Goldstein & Leib (1989) in that it is an integro–differential equation with cubic nonlinearity, but the structure of the nonlinear kernel function is now somewhat different from theirs. While the phenomenon is of most importance in supersonic shear layers, we restrict the analysis to the incompressible case because the nonlinear critical-layer dynamics are unaffected by compressibility effects, and their inclusion would greatly complicate the analysis. Moreover, the final amplitude equation (3.69), which is the principal result of this paper, remains valid for the compressible case. This equation has to be solved numerically, which is accomplished by using a fourth-order predictor–corrector scheme to integrate in the downstream direction, starting from the upstream linear state which is prescribed far upstream in the flow (relative to the streamwise lengthscale of the nonlinear region).

The calculated instability wave amplitudes initially follow the prescribed linear growth, but soon begin to either saturate or increase their rate of growth when the nonlinear effects come into play. Cumulative history effects eventually counteract the former trend, causing a rapid increase in amplitude which ends in a singularity at a finite downstream distance. The local asymptotic solution of the amplitude equation is derived. It shows that the flow will become fully nonlinear everywhere in

the shear layer and that the motion will then be governed by the full three-dimensional Euler's equations in the next stage of evolution downstream of the weakly nonlinear region.

The overall plan of the paper is as follows. The problem is formulated in §2, where we show how the nonlinear critical layer gradually evolves from the strictly linear finite growth rate solution. The flow outside the critical layer is a linear, unsteady three-dimensional perturbation about the two-dimensional mean shear-layer flow, which can be treated as locally parallel on the streamwise lengthscale over which the nonlinear effects take place. The latter occur entirely within the critical layer to the order of approximation of the analysis and determine the unknown amplitude function in the external solution. The transverse velocity fluctuation is taken as the basic variable for the external flow, and the (linear) equation for this quantity is expressed in terms of the 'Squire coordinates' associated with either of the two oblique modes.

We introduce a 'slowly varying' amplitude function, which depends on the streamwise coordinate through an appropriately scaled variable and is ultimately determined by the nonlinear flow in the critical layer, which we analyse in §3. Matching with the linear external instability waves leads to the nonlinear integro–differential equation that determines the amplitude of those waves. The numerical and asymptotic solutions to this equation are discussed in §5.

2. Formulation and solution outside the critical layer

We are concerned with a nearly inviscid incompressible shear flow between two parallel streams with nominally uniform velocities $U^{(1)} > U^{(2)}$. The upstream flow consists of a steady two-dimensional shear layer and a pair of oblique (i.e. three-dimensional) spatially growing (i.e. time harmonic) instability waves with the same frequency and streamwise wavenumbers but with equal and opposite (real) spanwise wavenumbers. The streamwise, transverse, and spanwise coordinates (x, y and z, respectively), the time t and all velocities are normalized by $\delta_0, \delta_0/\Delta$, and Δ, respectively, where δ_0 is half the mean shear-layer momentum thickness and

$$\Delta = \tfrac{1}{2}(U^{(1)} - U^{(2)}) \tag{2.1}$$

is a measure of the velocity difference across the shear layer. When nonlinear effects do not first intervene, the gradual viscous spreading of the mean shear layer causes the common spatial growth rate of the two linear instability waves to gradually decrease until they approach their common neutral stability point, whose Strouhal number and streamwise and (real) spanwise wavenumbers we denote by S_0, α, and $\pm\beta$, respectively.

As already indicated, nonlinear effects first become important at the streamwise position (upstream of the linear neutral stability point) where the local Strouhal number S (frequency normalized by Δ/δ_0) is

$$S = S_0 + \epsilon^{\frac{1}{3}} S_1. \tag{2.2}$$

Here $S_1 < 0$ is assumed to be an $O(1)$-constant, and ϵ denotes the characteristic amplitude of the instability wave in this region. The instability wave growth rate, which is also $O(\epsilon^{\frac{1}{3}})$, will then be determined by the nonlinear critical-layer effects. Finally, we require that the origin of the spatial coordinates x, y, z be located within this nonlinear region.

The transverse velocity fluctuations of the two upstream linear instability waves will then be of the form

$$-\bar{\alpha}(e^{i\beta z}+e^{-i\beta z})\,\mathrm{Re}\,ia^{\dagger}\phi_1^{(1)}(y)\,e^{i(\alpha\xi-\epsilon^{\frac{1}{3}}S_1 t)-\frac{1}{2}S_1 U_c'\bar{\kappa}x_1},$$

where t denotes the time,

$$\bar{\alpha}\equiv(\alpha^2+\beta^2)^{\frac{1}{2}}, \tag{2.3}$$

$\pm\beta$ denote the (real) spanwise wavenumbers of each of the individual instability waves and $\pm\theta$, where

$$\theta\equiv\tan^{-1}\frac{\beta}{\alpha}, \tag{2.4}$$

denotes the direction of propagation (relative to the mean flow direction) of these waves at their common neutral state.

$$\xi\equiv x-U_c t \tag{2.5}$$

is a streamwise coordinate in a reference frame moving downstream with the neutral phase velocity

$$U_c=\frac{S_0}{\alpha}, \tag{2.6}$$

$$x_1\equiv\epsilon^{\frac{1}{3}}x \tag{2.7}$$

is a scaled streamwise coordinate (in the fixed reference frame) and,

$$iS_1 U_c'\tfrac{1}{2}\bar{\kappa}$$

is a scaled complex wavenumber whose imaginary part is minus the common growth rate of the linear near neutral instability waves. $\Phi_1^{(1)}(y)$ is an appropriate solution of Rayleigh's equation, which can be taken as the neutral solution to the required order of approximation. The complex constant $a^{\dagger}$ is a measure of the complex (scaled) amplitude of the two waves.

The normalized pressure is denoted by p and the normalized velocity components in the moving $\{\xi,y,z\}$ coordinate system by $\{u,v,w\}$. We expect the solution outside the critical layer to expand like

$$u=U(y)+\epsilon u_1+\epsilon^{\frac{4}{3}}u_2+\ldots, \tag{2.8}$$

$$v=\epsilon v_1+\epsilon^{\frac{4}{3}}v_2+\ldots, \tag{2.9}$$

$$w=\epsilon w_1+\epsilon^{\frac{4}{3}}w_2+\ldots, \tag{2.10}$$

$$p=\epsilon p_1+\epsilon^{\frac{4}{3}}p_2+\ldots, \tag{2.11}$$

where $U(y)+U_c$ is the base-flow velocity, and the form of the upstream linear solution suggests that v_1 can be written as

$$v_1=-\bar{\alpha}(e^{i\beta z}+e^{-i\beta z})\,\mathrm{Re}\,i\Phi_1^{(1)}(y)A^{\dagger}(x_1)\,e^{i\alpha\zeta}, \tag{2.12}$$

where

$$\zeta\equiv\xi-S_1\epsilon^{\frac{1}{3}}t/\alpha, \tag{2.13}$$

and $A^{\dagger}$ is a function of the slow streamwise variable x_1, which will ultimately be determined by the nonlinear flow in the critical layer, but matching with the upstream linear instability waves requires that it satisfy the upstream boundary condition

$$A^{\dagger}\to a^{\dagger}e^{-S_1 U_c'\bar{\kappa}x_1/2}\quad\text{as}\quad x_1\to-\infty. \tag{2.14}$$

The $O(\epsilon^{\frac{4}{3}})$ terms (in (2.8)–(2.11)) are induced by nonlinear effects within the critical layer and by derivatives of the $O(\epsilon)$ terms with respect to x_1. They are, therefore, at

least in part, associated with linear growth rate effects. In fact, the entire solution (2.9) satisfies linear dynamics to the indicated order and is therefore determined by Rayleigh's equation

$$\left(\frac{\partial}{\partial t}+U\frac{\partial}{\partial \xi}\right)\nabla^2 v - U''\frac{\partial v}{\partial \xi}=0, \tag{2.15}$$

where the primes denote differentiation with respect to y and

$$\nabla^2 \equiv \frac{\partial^2}{\partial \xi^2}+\frac{\partial^2}{\partial y^2}+\frac{\partial^2}{\partial z^2} \tag{2.16}$$

is the Laplacian in the moving reference frame. It follows that v_2 is a function of the form $v_2(\zeta, x_1, y, z)$ and therefore satisfies

$$(U\nabla^2-U'')\frac{\partial v_2}{\partial \zeta}=-\left(2U\frac{\partial^2}{\partial \zeta^2}-U''\right)\frac{\partial v_1}{\partial x_1}+\left[\frac{S_1}{\alpha}\frac{\partial}{\partial \zeta}-(U+U_c)\frac{\partial}{\partial x_1}\right]\nabla^2 v_1, \tag{2.17}$$

where ∇^2 now denotes the Laplacian with respect to ζ, y, and z, and the partial derivatives with respect to ζ are at constant x_1 and vice versa. It follows from continuity that

$$\frac{\partial u_2}{\partial \zeta}+\frac{\partial v_2}{\partial y}+\frac{\partial w_2}{\partial z}+\frac{\partial u_1}{\partial x_1}=0. \tag{2.18}$$

$\Phi_1^{(1)}$ must, of course, satisfy the reduced Rayleigh's equation

$$\mathrm{L}^{(1)}\Phi_1^{(1)}=0, \tag{2.19}$$

where

$$\mathrm{L}^{(1)} \equiv \frac{\mathrm{d}^2}{\mathrm{d}y^2}-\left(\bar{\alpha}^2+\frac{U''}{U}\right) \tag{2.20}$$

denotes the reduced Rayleigh's operator, and u_1 and w_1 are then given by

$$u_1=(\mathrm{e}^{\mathrm{i}\beta z}+\mathrm{e}^{-\mathrm{i}\beta z})\cos\theta\,\mathrm{Re}\left[\Phi_1^{(1)\prime}(y)+\tan^2\theta\frac{U'(y)}{U(y)}\Phi_1^{(1)}(y)\right]A^{\dagger}(x_1)\,\mathrm{e}^{\mathrm{i}\alpha\zeta}+\mathrm{Re}\,F_{1\pm}^{(0)}(y,x_1)\,\mathrm{e}^{2\mathrm{i}\beta z}, \tag{2.21}$$

and

$$w_1=-2\sin\theta\sin\beta z\;\mathrm{Re}\,\mathrm{i}\left(\frac{U'}{U}\Phi_1^{(1)}-\Phi_1^{(1)\prime}\right)A^{\dagger}\mathrm{e}^{\mathrm{i}\alpha\zeta}, \tag{2.22}$$

where the ζ-independent term in (2.21), which is governed by linear dynamics in the main shear layer, is induced by nonlinear effects in the critical layer.

Then, since u_2, v_2, and w_2 have the same ζ-periodicity as v_1, they must be expressible in the form

$$u_2=\mathrm{Re}\sum_{m=0}^{\infty}F_2^{(m)}(y,z,x_1)\,\mathrm{e}^{\mathrm{i}m\alpha\zeta}, \tag{2.23}$$

$$v_2=-\bar{\alpha}\,\mathrm{Re}\,\mathrm{i}\sum_{m=0}^{\infty}\tilde{\Phi}_2^{(m)}(y,z,x_1)\,\mathrm{e}^{\mathrm{i}m\alpha\zeta}, \tag{2.24}$$

$$w_2=\mathrm{Re}\sum_{m=0}^{\infty}H_2^{(m)}(y,z,x_1)\,\mathrm{e}^{\mathrm{i}m\alpha\zeta}. \tag{2.25}$$

Substituting (2.12) and (2.24) into (2.17) we find that

$$\tilde{\Phi}_2^{(1)}=2\cos\beta z\,\Phi_2^{(1)}(y,x_1), \tag{2.26}$$

where $\Phi_2^{(1)}$ satisfies

$$i\alpha U\mathrm{L}^{(1)}\Phi_2^{(1)} = \left[\left(iS_1 - U_c\frac{d}{dx_1}\right)A^\dagger\right](\Phi_1^{(1)\prime\prime} - \bar{\alpha}^2\Phi_1^{(1)}) + 2\alpha^2 U\frac{dA^\dagger}{dx_1}\Phi_1^{(1)}. \tag{2.27}$$

It now follows from (2.23)–(2.25) and (2.18) that

$$F_2^{(1)} = (\sec\theta\bar{F}_2^{(1)} + \sin\theta\tan\theta\bar{H}_2^{(1)})(e^{i\beta z} + e^{-i\beta z}), \tag{2.28}$$

and

$$H_2^{(1)} = -\sin\theta\bar{H}_2^{(1)}(e^{i\beta z} - e^{-i\beta z}), \tag{2.29}$$

where $\bar{F}_2^{(1)}$ is given by

$$\bar{F}_2^{(1)} = \Phi_2^{(1)\prime} - \frac{\cos^2\theta}{i\alpha}\left(\Phi_1^{(1)\prime} + \tan^2\theta\frac{U'}{U}\Phi_1^{(1)}\right)\frac{dA^\dagger}{dx_1}, \tag{2.30}$$

and $\bar{H}_2$ can be defined similarly, but will not be needed in the following analysis.

Equations (2.19) and (2.27) must, in general, be solved numerically. Fortunately, we need only know the local behaviour of their solutions at the critical level where $U(y) = 0$. This will occur at the inflection point $U''(y_c) = 0$, or

$$U_c'' = 0 \tag{2.31}$$

(where the subscript c is used to denote quantities at the critical level) provided we assume, as we now do, that $U(y)$ has only a single inflection point.

The critical level, which we can always suppose to lie at $y = 0$, is then a regular point for the operator (2.20), and (2.19) will, therefore, possess the two linearly independent solutions

$$\tilde{\Phi}^{(1)} = 1 + \frac{1}{2!}\left(\bar{\alpha}^2 + \frac{U_c'''}{U_c'}\right)y^2 + \ldots \tag{2.32}$$

and

$$\tilde{\Phi}^{(2)} = y + \frac{1}{3!}\left(\bar{\alpha}^2 + \frac{U_c'''}{U_c'}\right)y^3 + \ldots \tag{2.33}$$

as $y \to 0$.

Then we can put

$$\Phi_1^{(1)} = \tilde{\Phi}^{(1)} + b_1\tilde{\Phi}^{(2)}, \tag{2.34}$$

where b_1 is a constant which must, in general, be determined along with $\bar{\alpha}$ by solving (2.19) numerically subject to the proper boundary conditions at $y = \pm\infty$. Then (2.21) and (2.22) imply that

$$u_1 = \cos\theta(e^{i\beta z} + e^{-i\beta z})\left\{\frac{\tan^2\theta}{y} + b_1(1 + \tan^2\theta) + \left[\bar{\alpha}^2(1 + \tfrac{1}{2}\tan^2\theta) + \frac{U_c'''}{U_c'}(1 + \tfrac{5}{6}\tan^2\theta)\right]y\right\}\mathrm{Re}\,A^\dagger e^{i\alpha\zeta} + \mathrm{Re}\,F_{1\pm}^{(0)}(0, x_1)e^{2i\beta z} + \ldots, \tag{2.35}$$

$$v_1 = -\bar{\alpha}(e^{i\beta z} + e^{-i\beta z})\,\mathrm{Re}\,iA^\dagger e^{i\alpha\zeta} + \ldots, \tag{2.36}$$

$$w_1 = -2\sin\theta\sin\beta z\left[\frac{1}{y} - \frac{1}{2}\left(\bar{\alpha}^2 + \frac{1}{3}\frac{U_c'''}{U_c'}\right)y\right]\mathrm{Re}\,iA^\dagger e^{i\alpha\zeta} + \ldots \tag{2.37}$$

as $y \to 0$, where we have anticipated the fact that the critical-layer solution produces an $O(\epsilon)$ mean flow change across the critical layer but no change in the second harmonic of the streamwise velocity fluctuation.

It follows from (2.27), (2.32), and (2.33) that there exist two continuous functions, say $\Phi_{P,1}$ and $\Phi_{P,2}$, which satisfy

$$\mathrm{L}^{(1)}\Phi_{P,1} = \frac{U''}{U^2}\Phi_1^{(1)} \tag{2.38}$$

and

$$\mathrm{L}^{(1)}\Phi_{P,2} = \Phi_1^{(1)} \tag{2.39}$$

but are, in general, unbounded at $y = \pm\infty$. $\Phi_{P,1}$ will behave like

$$\tilde{e}_1 + \tilde{e}_{2,L}\, y \ln|y| + \tilde{e}_2 y + \ldots,$$

as $y \to 0$ and $\Phi_{P,2}$ will be regular there. The relevant solution to 2.27) must then be of the form

$$\Phi_2^{(1)} = \frac{\mathrm{i}}{\alpha}\left(U_c A^{\dagger}_{x_1} - \mathrm{i}S_1 A^{\dagger}\right)\left(\Phi_{P,1} - c^{\pm}_{2,1}\tilde{\Phi}^{(1)} - b^{\pm}_{2,1}\tilde{\Phi}^{(2)}\right)$$
$$-2\mathrm{i}\alpha A^{\dagger}_{x_1}\left(\Phi_{P,2} - c^{\pm}_{2,2}\tilde{\Phi}^{(1)} - b^{\pm}_{2,2}\tilde{\Phi}^{(2)}\right), \tag{2.40}$$

where $b^{\pm}_{2,n}, c^{\pm}_{2,n}$ are real constants (even on the slow scale x_1), which must, in general, be determined numerically.

It now follows from (2.30) that

$$\bar{F}_2^{(1)} = -\frac{\sin^2\theta}{\mathrm{i}\alpha y}A^{\dagger}_{x_1} + e_1(x_1) + e_2(x_1)\ln|y| + 2\mathrm{i}\alpha A^{\dagger}_{x_1} b^{\pm}_{2,2}$$
$$-\frac{\mathrm{i}}{\alpha}\left(U_c A^{\dagger}_{x_1} - \mathrm{i}S_1 A^{\dagger}\right)b^{\pm}_{2,1} + \ldots \quad \text{as} \quad y \to \pm 0, \tag{2.41}$$

where the specific values of e_1 and e_2 are immaterial, and we do not need the corresponding expressions for $\bar{H}_2^{(1)}$ in the following analysis.

3. The critical layer

Equations (2.35) and (2.37) cleary show that the outer expansion (2.8)–(2.11) becomes singular at the critical level. The linear small growth rate critical-layer thickness is of the order of the linear growth rate which is $O(\epsilon^{\frac{1}{3}})$ in the present case. The appropriate scaled transverse coordinate in this region is therefore

$$Y = \frac{y}{\epsilon^{\frac{1}{3}}}. \tag{3.1}$$

Introducing this along with (2.12), (2.23) to (2.25), (2.40), (2.41), and (2.32)–(2.37) into (2.8)–(2.11) and re-expanding the result suggests that the critical-layer solution should expand like

$$u = \epsilon^{\frac{1}{3}}U_c' Y + \epsilon^{\frac{2}{3}}\hat{u}_0 + \epsilon\hat{u}_1 + \epsilon^{\frac{4}{3}}\hat{u}_2 + \ldots, \tag{3.2}$$

$$\bar{v} = -\epsilon^{\frac{2}{3}}\bar{\alpha}(\mathrm{e}^{\mathrm{i}\beta z} + \mathrm{e}^{-\mathrm{i}\beta z})\,\mathrm{Re}\,\mathrm{i}A^{\dagger}\mathrm{e}^{\mathrm{i}\alpha\zeta} + \epsilon\hat{v}_1 + \epsilon^{\frac{4}{3}}\hat{v}_2 + \ldots, \tag{3.3}$$

$$w = \epsilon^{\frac{2}{3}}\hat{w}_0 + \epsilon\hat{w}_1 + \epsilon^{\frac{4}{3}}\hat{w}_2 + \ldots, \tag{3.4}$$

$$p = \epsilon\hat{p}_0 + \epsilon^{\frac{4}{3}}\hat{p}_1 + \epsilon^{\frac{5}{3}}\hat{p}_2 + \ldots, \tag{3.5}$$

where we suppose that the $\epsilon^n \ln\epsilon$ terms have been incorporated in the $\hat{u}_0$, $\hat{u}_1$, etc.,

$$\hat{p}_0 = U_c' \cos\theta(\mathrm{e}^{\mathrm{i}\beta z} + \mathrm{e}^{-\mathrm{i}\beta z})\,\mathrm{Re}\,A^{\dagger}\mathrm{e}^{\mathrm{i}\alpha\zeta}, \tag{3.6}$$

and, for convenience, we have put

$$\bar{v} \equiv \epsilon^{-\frac{1}{3}} v. \tag{3.7}$$

The $\hat{u}_n$, $\hat{v}_n$, $\hat{w}_n$, etc. are functions of ζ, Y, z, and x_1, only and are determined by the inviscid momentum and continuity equations. It follows from (2.23), (2.25), (2.28), and (2.41) that matching with the external solution requires that

$$\frac{\alpha\beta}{2\pi^2}\int_0^{2\pi/\alpha}\int_0^{2\pi/\beta} \mathrm{e}^{-\mathrm{i}(\alpha\zeta+\beta z)}\Delta\bar{u}_2^+(\zeta,z,x_1)\,\mathrm{d}z\,\mathrm{d}\zeta = 2\mathrm{i}\alpha A^+_{x_1}(b^+_{2,2}-b^-_{2,2})$$

$$-\frac{\mathrm{i}}{\alpha}(U_{\mathrm{c}}A^+_{x_1}-\mathrm{i}S_1A^+)(b^+_{2,1}-b^-_{2,1}), \tag{3.8}$$

where we have put

$$\Delta\bar{u}_2^+ \equiv \lim_{Y\to\infty}[\bar{u}_2^+(\zeta,Y,z,x_1)-\bar{u}_2^+(\zeta,-Y,z,x_1)] \tag{3.9}$$

and

$$\bar{u}_n^{\pm} \equiv \hat{u}_n\cos\theta \pm \hat{w}_n\sin\theta \quad \text{for} \quad n=0,1,2,\ldots. \tag{3.10}$$

The requirement (3.8) merely states that the change in propagation-direction velocity across the critical layer, as calculated from within, is equal to the change in that velocity as calculated from the linear external solution.

It turns out to be convenient to work in terms of the spanwise vorticity

$$\omega \equiv \frac{\partial v}{\partial x}-\frac{\partial u}{\partial y}, \tag{3.11}$$

which expands like

$$\omega = -U_{\mathrm{c}}'-\epsilon^{\frac{1}{3}}\hat{u}_{0Y}-\epsilon^{\frac{2}{3}}\hat{u}_{1Y}+\epsilon\omega_2+\ldots, \tag{3.12}$$

where

$$\omega_2 \equiv -\hat{u}_{2Y}+\bar{\alpha}\alpha(\mathrm{e}^{\mathrm{i}\beta z}+\mathrm{e}^{-\mathrm{i}\beta z})\,\mathrm{Re}\,A^+\mathrm{e}^{\mathrm{i}\alpha\zeta}. \tag{3.13}$$

Then ω and

$$\boldsymbol{u} \equiv \{u,\bar{v},w\} \tag{3.14}$$

satisfy

$$\left[\left(u-\epsilon^{\frac{1}{3}}\frac{S_1}{\alpha}\right)\frac{\partial}{\partial\zeta}+\bar{v}\frac{\partial}{\partial Y}+\epsilon^{\frac{1}{3}}(u+U_{\mathrm{c}})\frac{\partial}{\partial x_1}+w\frac{\partial}{\partial z}\right]\omega = \frac{1}{\epsilon^{\frac{1}{3}}}u_z w_Y+\omega w_z-\epsilon^{\frac{1}{3}}\bar{v}_z w_\zeta-\epsilon^{\frac{2}{3}}\bar{v}_z w_{x_1}, \tag{3.15}$$

$$\left[\left(u-\epsilon^{\frac{1}{3}}\frac{S_1}{\alpha}\right)\frac{\partial}{\partial\zeta}+\bar{v}\frac{\partial}{\partial Y}+\epsilon^{\frac{1}{3}}(u+U_{\mathrm{c}})\frac{\partial}{\partial x_1}+w\frac{\partial}{\partial z}\right]\boldsymbol{u} = -\left\{p_\zeta+\epsilon^{\frac{1}{3}}p_{x_1},\frac{1}{\epsilon^{\frac{2}{3}}}p_Y,p_z\right\}, \tag{3.16}$$

and

$$u_\zeta+\bar{v}_Y+w_z+\epsilon^{\frac{1}{3}}u_{x_1}=0. \tag{3.17}$$

Substituting the expansions (3.2)–(3.6) and (3.12) into (3.15) and (3.16), we find that

$$\mathscr{L}_0\hat{w}_0 = -U_{\mathrm{c}}'\bar{\alpha}\sin\theta\cos\theta\,\mathrm{Re}\,\mathrm{i}(\mathrm{e}^{\mathrm{i}\beta z}-\mathrm{e}^{-\mathrm{i}\beta z})A^+\mathrm{e}^{\mathrm{i}\alpha\zeta}, \tag{3.18}$$

$$\mathscr{L}_0\hat{w}_1 = \bar{\alpha}(\mathrm{e}^{\mathrm{i}\beta z}+\mathrm{e}^{-\mathrm{i}\beta z})(\mathrm{Re}\,\mathrm{i}A^+\mathrm{e}^{\mathrm{i}\alpha\zeta})\hat{w}_{0Y}-\left(\hat{u}_0\frac{\partial}{\partial\zeta}+\hat{w}_0\frac{\partial}{\partial z}\right)\hat{w}_0-U_{\mathrm{c}}'Y\hat{w}_{0x_1}-\hat{p}_{1z}, \tag{3.19}$$

$$\mathscr{L}_0\hat{u}_0 = U_{\mathrm{c}}'\bar{\alpha}\sin^2\theta(\mathrm{e}^{\mathrm{i}\beta z}+\mathrm{e}^{-\mathrm{i}\beta z})\,\mathrm{Re}\,\mathrm{i}A^+\mathrm{e}^{\mathrm{i}\alpha\zeta}, \tag{3.20}$$

$$\mathscr{L}_0\hat{u}_{1Y} = \bar{\alpha}(\mathrm{e}^{\mathrm{i}\beta z}+\mathrm{e}^{-\mathrm{i}\beta z})(\mathrm{Re}\,\mathrm{i}A^+\mathrm{e}^{\mathrm{i}\alpha\zeta})\hat{u}_{0YY}+(\hat{u}_0\hat{w}_{0z}-\hat{u}_{0z}\hat{w}_0)_Y+U_{\mathrm{c}}'(\hat{w}_{1z}-Y\hat{u}_{0x_1Y}), \tag{3.21}$$

$$\mathscr{L}_0\hat{q}_2 = \bar{\alpha}(\mathrm{e}^{\mathrm{i}\beta z}+\mathrm{e}^{-\mathrm{i}\beta z})(\mathrm{Re}\,\mathrm{i}A^{\dagger}\mathrm{e}^{\mathrm{i}\alpha\zeta})(\bar{u}^{+}_{1YY}-\cos\theta U_{\mathrm{c}}''' Y)-\frac{U_{\mathrm{c}}'''}{U_{\mathrm{c}}'}(\mathrm{e}^{\mathrm{i}\beta z}+\mathrm{e}^{-\mathrm{i}\beta z})$$
$$\times\,\mathrm{Re}\,(U_{\mathrm{c}}A^{+}_{x_1}-\mathrm{i}S_1A^{\dagger})\,\mathrm{e}^{\mathrm{i}\alpha\zeta}+(\bar{u}_1^{-}\hat{w}_{0z}-\hat{u}_0\bar{u}^{+}_{1\zeta}-\hat{w}_0\bar{u}^{+}_{1z}-\hat{w}_1\cos\theta\hat{u}_{0z}$$
$$-\hat{u}_1\sin\theta\hat{w}_{0\zeta}-\hat{v}_1\bar{u}^{+}_{0Y})_Y+U_{\mathrm{c}}'(\cos\theta\hat{w}_{2z}-\sin\theta\hat{w}_{2\zeta}-\sin\theta\hat{w}_{1x_1}-Y\bar{u}^{+}_{1x_1Y})-(\hat{u}_0\bar{u}^{+}_{0x_1})_Y, \tag{3.22}$$

and
$$\hat{v}_{1Y} = -\hat{u}_{1\zeta}-\hat{w}_{1z}-\hat{u}_{0x_1}, \tag{3.23}$$

where we have put
$$\mathscr{L}_0 \equiv U_{\mathrm{c}}\frac{\partial}{\partial x_1}+\left(U_{\mathrm{c}}'Y-\frac{S_1}{\alpha}\right)\frac{\partial}{\partial\zeta},$$

and
$$\hat{q}_2 \equiv -\omega_2\cos\theta+\sin\theta\,(\hat{w}_{2Y}+2\bar{\alpha}\beta\sin\beta z\,\mathrm{Re}\,\mathrm{i}A^{\dagger}\mathrm{e}^{\mathrm{i}\alpha\zeta})-\frac{U_{\mathrm{c}}'''}{U_{\mathrm{c}}'}(\mathrm{e}^{\mathrm{i}\beta z}+\mathrm{e}^{-\mathrm{i}\beta z})\,\mathrm{Re}\,A^{\dagger}\mathrm{e}^{\mathrm{i}\alpha\zeta}, \tag{3.24}$$

and matching with the outer solution shows that $\hat{q}_2$ and $\bar{u}_{1Y}-\frac{1}{2}U_{\mathrm{c}}'''\cos\theta Y^2$ go to zero as $Y\to\pm\infty$.

It is now convenient to introduce the following normalized variables:

$$\bar{x} \equiv -\tfrac{1}{2}S_1U_{\mathrm{c}}'x_1-x_0, \tag{3.25}$$

$$\eta \equiv -2\alpha\left(Y-\frac{S_1}{\alpha U_{\mathrm{c}}'}\right)\Big/S_1U_{\mathrm{c}}, \tag{3.26}$$

$$X \equiv \alpha\zeta-X_0, \tag{3.27}$$

and
$$A \equiv 4A^{\dagger}\alpha^2\mathrm{e}^{\mathrm{i}X_0}/(S_1U_{\mathrm{c}})^2U_{\mathrm{c}}', \tag{3.28}$$

where x_0 and X_0 are real constants.

Then (3.18) and (3.20) can be integrated immediately to obtain

$$\hat{u}_0 = -U_{\mathrm{c}}U_{\mathrm{c}}'\frac{S_1}{\alpha}\sin\theta\tan\theta\cos\beta z\,\mathrm{Re}\,\mathrm{i}W_1^{(0)}\mathrm{e}^{\mathrm{i}X}, \tag{3.29}$$

$$\hat{w}_0 = -\frac{U_{\mathrm{c}}U_{\mathrm{c}}'S_1}{\alpha}\sin\theta\sin\beta z\,\mathrm{Re}\,W_1^{(0)}\mathrm{e}^{\mathrm{i}X}, \tag{3.30}$$

where we have put
$$W_1^{(0)} = \int_{-\infty}^{\bar{x}}\mathrm{e}^{-\mathrm{i}\eta(\bar{x}-\tilde{x})}A(\tilde{x})\,\mathrm{d}\tilde{x}. \tag{3.31}$$

It is worth noticing that
$$W_1^{(0)} \to \frac{\mathrm{i}}{\eta-\mathrm{i}\bar{\kappa}}\mathrm{e}^{\bar{\kappa}\bar{x}}$$

when
$$A \to \mathrm{e}^{\bar{\kappa}\bar{x}}$$

so that (3.29) approaches the linear critical-layer solution (given by the generalization of equation (4.34) in Goldstein & Leib 1988) when $A^{\dagger}$ approaches the linear upstream condition (2.14).

Equations (3.19) and (3.21) clearly possess solutions of the form

$$\hat{u}_{1Y} = \tfrac{1}{2}U_{\mathrm{c}}'''Y^2-\tfrac{1}{2}\sin\theta U_{\mathrm{c}}'\sum_{n,m=-2}^{2}Q^{(1)}_{n,m}(\eta,\bar{x})\,\mathrm{e}^{\mathrm{i}(nX+m\beta z)}, \tag{3.32}$$

and
$$\hat{w}_1 = \frac{1}{4\alpha}S_1U_{\mathrm{c}}U_{\mathrm{c}}'\sin\theta\sum_{n,m=-2}^{2}W^{(1)}_{n,m}(\eta,\bar{x})\,\mathrm{e}^{\mathrm{i}(nX+m\beta z)}, \tag{3.33}$$

where the first term in (3.32) was inserted to ensure that $Q^{(1)}_{n,m} \to 0$ as $\eta \to \pm\infty$ for all n, m.

Substituting (3.32) and (3.33) along with (3.29) and (3.30) into (3.19) and (3.21) shows that

$$\mathrm{L}_0 W^{(1)}_{0,2} = \mathrm{i}\sec\theta(2\sin^2\theta|W^{(0)}_1|^2 - \mathrm{Im}\, A^* W^{(0)}_{1\eta}), \tag{3.34}$$

$$\mathrm{L}_2 W^{(1)}_{2,0} = 0, \tag{3.35}$$

$$\mathrm{L}_2 Q^{(1)}_{2,0} = \tan\theta\sec\theta\,(A W^{(0)}_{1\eta\eta} - 4\mathrm{i}\sin^2\theta W^{(0)}_1 W^{(0)}_{1\eta}), \tag{3.36}$$

where the asterisk denotes the complex conjugate, and we have put

$$\mathrm{L}_n \equiv \frac{\partial}{\partial\bar{x}} + \mathrm{i}n\eta \quad \text{for} \quad n = 0, 1, 2, \ldots, \tag{3.37}$$

and in writing down (3.36) we have anticipated the fact that the relevant solution to (3.35) is the trivial solution

$$W^{(1)}_{2,0} = 0. \tag{3.38}$$

Inserting (3.31) into (3.34) and (3.36) and integrating yield

$$W^{(1)}_{0,2} = \mathrm{i}\sec\theta\,\mathrm{Re}\int_{-\infty}^{\bar{x}} A^*(\tilde{x})\,\mathrm{e}^{-\mathrm{i}\eta\tilde{x}}[I_1(\tilde{x}) + 4\sin^2\theta(\bar{x}-\tilde{x})I_0(\tilde{x})]\,\mathrm{d}\tilde{x} \tag{3.39}$$

and

$$Q^{(1)}_{2,0} = -\tan\theta\sec\theta\,\mathrm{e}^{-2\mathrm{i}\eta\bar{x}}\left[\int_{-\infty}^{\bar{x}} A(\tilde{x})\,\mathrm{e}^{\mathrm{i}\eta\tilde{x}} I_2(\tilde{x})\,\mathrm{d}\tilde{x} + 2\sin^2\theta I_1^2(\bar{x})\right], \tag{3.40}$$

where we have put

$$I_n(x) \equiv \int_{-\infty}^{x} \mathrm{e}^{\mathrm{i}\eta\tilde{x}}(x-\tilde{x})^n A(\tilde{x})\,\mathrm{d}\tilde{x} \quad \text{for} \quad n = 0, 1, 2, \ldots. \tag{3.41}$$

Inserting (3.39) along with (3.29)–(3.33) into (3.21) and integrating we obtain

$$Q^{(1)}_{0,2} = \tan\theta\sec\theta\,\mathrm{Re}\int_{-\infty}^{\bar{x}} A^*(\tilde{x})\,\mathrm{e}^{-\mathrm{i}\eta\tilde{x}}[I_2(\tilde{x}) - 2(\bar{x}-\tilde{x})I_1(\tilde{x}) - 4(\bar{x}-\tilde{x})^2\sin^2\theta I_0(\tilde{x})]\,\mathrm{d}\tilde{x}. \tag{3.42}$$

Since $\hat{u}_{1Y}$ and $\hat{w}_1$ are real we must set

$$W^{(1)}_{0,-2} = W^{(1)*}_{0,2}, \tag{3.43}$$

$$Q^{(1)}_{0,-2} = Q^{(1)*}_{0,2}, \tag{3.44}$$

$$W^{(1)}_{-2,0} = W^{(1)*}_{2,0} = 0, \tag{3.45}$$

and

$$Q^{(1)}_{-2,0} = Q^{(1)*}_{2,0}. \tag{3.46}$$

It is easy to show that

$$Q^{(1)}_{0,0}\cos\theta + W^{(1)}_{0,0\eta}\sin\theta = \tan\theta\,\mathrm{Re}\int_{-\infty}^{\bar{x}} A^*(\tilde{x})\,\mathrm{e}^{-\mathrm{i}\eta\tilde{x}} I_2(\tilde{x})\,\mathrm{d}\tilde{x}, \tag{3.47}$$

$$Q^{(1)}_{1,1} = \frac{\mathrm{i}}{2\alpha} S_1 U_{\mathrm{c}}' \sin\theta W^{(0)}_{1\eta\bar{x}}, \tag{3.48}$$

and

$$\left[W^{(1)}_{1,1}\sin\theta - \frac{2Y\alpha}{S_1 U_{\mathrm{c}}}(Q^{(1)}_{1,1}\cos\theta + W^{(1)}_{1,1\eta}\sin\theta)\right]_{\bar{x}} = \hat{C}\mathrm{L}_1\left(W^{(1)}_{1,1} - \frac{\mathrm{i}}{2\alpha} S_1 U_{\mathrm{c}}' W^{(0)}_{1\bar{x}}\right)_{\eta} \tag{3.49}$$

where $\hat{C}$ is a constant whose specific value will not affect our analysis. The remaining Q and W can be similarly determined, but are not used in the following analysis.

It now follows from (3.32) and (3.33) that (3.22) possesses a solution of the form

$$\hat{q}_2 = -\tfrac{1}{2}\sin\theta U_c' \sum_{n,\,m=-3}^{3} Q^{(2)}_{n,m}(\eta,\bar{x})\,\mathrm{e}^{\mathrm{i}(nX+m\beta z)}, \tag{3.50}$$

where
$$Q^{(2)}_{n,m} \to 0 \quad \text{as} \quad \eta \to \pm\infty. \tag{3.51}$$

Substituting this along with (3.32), (3.33), (3.48), (3.38), and (3.43)–(3.46) into (3.22) and (3.23) yields

$$\begin{aligned} \mathrm{L}_1\left[Q^{(2)}_{1,1} - \hat{C}\left(W^{(1)}_{1,1} - \frac{\mathrm{i}}{2\alpha}S_1 U_c' W^{(0)}_{1\bar{x}}\right)_\eta\right] &= \tfrac{1}{2}\mathrm{i}\{A[Q^{(1)}_{0,2} + Q^{(1)}_{0,0} + \tan\theta(W^{(1)}_{0,2} + W^{(1)}_{0,0})_\eta]_\eta \\ &\quad - A^* Q^{(1)}_{2,0\eta}\} + 2\sin^2\theta\frac{\partial}{\partial\eta}(W^{(0)}_1 U^{(1)}_{0,2} - W^{(0)}_{1\eta} V^{(1)}_{0,2} + W^{(0)*}_{1\eta} V^{(1)}_{2,0}) \\ &\quad + \frac{U_c S_1^2}{2\alpha^2\sin\theta}\left(\frac{U_c'''}{U_c'^2}\right)(\tfrac{1}{2}U_c U_c' A_{\bar{x}} + \mathrm{i}A), \end{aligned} \tag{3.52}$$

where
$$U^{(1)}_{0,2\eta} = Q^{(1)}_{0,2}, \tag{3.53}$$

$$V^{(1)}_{0,2\eta} = \tan\theta W^{(1)}_{0,2}, \tag{3.54}$$

and
$$V^{(1)}_{2,0\eta\eta} = Q^{(1)}_{2,0}. \tag{3.55}$$

Inserting (3.39) and (3.42), we find that

$$R_{0,2} \equiv 2\sin^2\theta\frac{\partial}{\partial\eta}(W^{(0)}_1 U^{(1)}_{0,2} - W^{(0)}_{1\eta} V^{(1)}_{0,2}) = \sin\theta\tan^2\theta(W^{(0)}_1 J_{3\bar{x}} + 2W^{(0)}_{1\eta} J_{2\bar{x}\bar{x}} - W^{(0)}_{1\eta\eta} J_{1\bar{x}\bar{x}\bar{x}}), \tag{3.56}$$

where the J_n depend on both $\bar{x}$ and η and are defined by

$$J_{1\eta} = \tfrac{1}{3}\mathrm{i}\,\mathrm{Re}\int_{-\infty}^{\bar{x}} A^*(\tilde{x})(\bar{x}-\tilde{x})^3\left[(\bar{x}-\tilde{x})\sin^2\theta + \mathrm{i}\frac{\partial}{\partial\eta}\right]\mathrm{e}^{-\mathrm{i}\eta\tilde{x}} I_0(\tilde{x})\,\mathrm{d}\tilde{x}, \tag{3.57}$$

$$J_2 = \mathrm{i}(J_1 - J_4), \tag{3.58}$$

where

$$J_4 \equiv \tfrac{2}{3}\sin^2\theta\,\mathrm{Re}\int_{-\infty}^{\bar{x}} A^*(\tilde{x})(\bar{x}-\tilde{x})^3\,\mathrm{e}^{-\mathrm{i}\eta\tilde{x}} I_0(\tilde{x})\,\mathrm{d}\tilde{x} + \frac{1}{2}\int_{-\infty}^{\bar{x}} A(\tilde{x})(\bar{x}-\tilde{x})^2\,\mathrm{e}^{\mathrm{i}\eta\tilde{x}} I_1^*(\tilde{x})\,\mathrm{d}\tilde{x}, \tag{3.59}$$

and

$$J_3 = -2\,\mathrm{Re}\int_{-\infty}^{\bar{x}} A^*(\tilde{x})(\bar{x}-\tilde{x})[\tfrac{4}{3}\sin^2\theta(\bar{x}-\tilde{x})^2 I_0(\tilde{x}) + (\bar{x}-\tilde{x})I_1(\tilde{x}) - I_2(\tilde{x})]\,\mathrm{e}^{-\mathrm{i}\eta\tilde{x}}\,\mathrm{d}\tilde{x}. \tag{3.60}$$

Then, upon integrating by parts and inserting (3.31), we obtain

$$\begin{aligned} \int_{-\infty}^{\bar{x}} \mathrm{e}^{-\mathrm{i}\eta(\bar{x}-\tilde{x})} R_{0,2}\,\mathrm{d}\tilde{x} &= \sin\theta\tan^2\theta\,\mathrm{e}^{-\mathrm{i}\eta\bar{x}}\{J_{1\bar{x}\bar{x}} I_2(\bar{x}) - 2J_{4\bar{x}} I_1(\bar{x}) \\ &\quad - \int_{-\infty}^{\bar{x}} \mathrm{e}^{\mathrm{i}\eta\tilde{x}} A(\tilde{x})[2J_4(\tilde{x}) - 2J_4(\bar{x}) + J_3(\tilde{x}) - J_3(\bar{x})]\,\mathrm{d}\tilde{x}\}. \end{aligned} \tag{3.61}$$

Substituting (3.40) into (3.55) we find after some manipulation that

$$V^{(1)}_{2,0} = -\tfrac{1}{2}\mathrm{i}\,\mathrm{e}^{-2\mathrm{i}\eta\bar{x}}\left(\frac{\partial}{\partial\bar{x}}\mathrm{e}^{2\mathrm{i}\eta\bar{x}} U^{(1)}_{2,0}\right) + \tfrac{1}{2}\tan\theta\sec\theta[A(\bar{x})\,\mathrm{e}^{-\mathrm{i}\eta\bar{x}} I_1(\bar{x}) + 2\sin^2\theta\,\mathrm{e}^{-2\mathrm{i}\eta\bar{x}} I_0^2(\bar{x})], \tag{3.62}$$

where
$$U^{(1)}_{2,0\eta} = Q^{(1)}_{2,0}. \tag{3.63}$$

Inserting this along with (3.31) into

$$\int_{-\infty}^{\bar{x}} \mathrm{e}^{-\mathrm{i}\eta(\bar{x}-\tilde{x})} R_{2,0}\,\mathrm{d}\tilde{x},$$

where
$$R_{2,0} \equiv 2\sin^2\theta \frac{\partial}{\partial\eta} W^{(0)*}_{1\eta} V^{(1)}_{2,0} \tag{3.64}$$

and integrating by parts now shows that

$$\int_{-\infty}^{\bar{x}} \mathrm{e}^{-\mathrm{i}\eta(\bar{x}-\tilde{x})} R_{2,0}\,\mathrm{d}\tilde{x} = \mathrm{i}\sin^2\theta\,\mathrm{e}^{\mathrm{i}\eta\bar{x}} I^*_2(\bar{x})\,U^{(1)}_{2,0}(\bar{x})$$
$$-\sin\theta\tan^2\theta\,\mathrm{e}^{-\mathrm{i}\eta\bar{x}} \int_{-\infty}^{\bar{x}} I^*_2(\tilde{x})\,[A(\tilde{x})\,\mathrm{e}^{\mathrm{i}\eta\tilde{x}} I_1(\tilde{x}) + 2\sin^2\theta I^2_0(\tilde{x})]\,\mathrm{d}\tilde{x}. \tag{3.65}$$

It is now easy to write down the solution to (3.52) by using (3.61), (3.65), (3.39), (3.42), and (3.47). Using the resulting formula for $Q^{(2)}_{1,1}$ and integrating by parts shows that

$$\frac{1}{2\pi}\int_{-\infty}^{\infty} Q^{(2)}_{1,1}\,\mathrm{d}\eta = \frac{U_\mathrm{c} S_1^2 U'''_\mathrm{c}}{4\alpha^2 \sin\theta U'^2_\mathrm{c}} (\tfrac{1}{2} U_\mathrm{c} U'_\mathrm{c} A_{\bar{x}} + \mathrm{i}A)$$
$$+\sec\theta\tan\theta \int_{-\infty}^{\bar{x}}\int_{-\infty}^{\tilde{x}} K(\bar{x}\,|\,\tilde{x},\tilde{x}_1)\,A(\tilde{x})\,A(\tilde{x}_1)\,A(\tilde{x}+\tilde{x}_1-\bar{x})\,\mathrm{d}\tilde{x}_1\,\mathrm{d}\tilde{x}, \tag{3.66}$$

where we have put

$$K(\bar{x}\,|\,\tilde{x},\tilde{x}_1) \equiv (\bar{x}-\tilde{x})\{[\tfrac{1}{2}(\bar{x}-\tilde{x}) + \sin^2\theta(\tilde{x}-\tilde{x}_1)]\,[2(\tilde{x}-\tilde{x}_1)-(\bar{x}-\tilde{x})]$$
$$-4\sin^4\theta[(\tilde{x}-\tilde{x}_1)^2 + (\bar{x}-\tilde{x})\,(\bar{x}-\tilde{x}_1)]\}. \tag{3.67}$$

It now follows from (3.8) and (3.24)–(3.28) that

$$\sin\theta\int_{-\infty}^{\infty} Q^{(2)}_{1,1}\,\mathrm{d}\eta = \tfrac{1}{2}\mathrm{i}S_1^2 U_\mathrm{c}\left[U'_\mathrm{c} A_{\bar{x}}(b^+_{2,2}-b^-_{2,2}) - \frac{1}{\alpha^2}(\tfrac{1}{2}U_\mathrm{c}U'_\mathrm{c}A_{\bar{x}} + \mathrm{i}A)\,(b^+_{2,1}-b^-_{2,1})\right] \tag{3.68}$$

Inserting (3.66) into this result yields

$$\frac{1}{\bar{\kappa}} A_{\bar{x}} = A + \gamma\tan^2\theta \int_{-\infty}^{\bar{x}}\int_{-\infty}^{\tilde{x}} K(\bar{x}\,|\,\tilde{x},\tilde{x}_1)\,A(\tilde{x})\,A(\tilde{x}_1)\,A^*(\tilde{x}+\tilde{x}_1-\bar{x})\,\mathrm{d}\tilde{x}_1\,\mathrm{d}\tilde{x}, \tag{3.69}$$

where
$$\frac{1}{\bar{\kappa}} = \gamma S_1^2 U_\mathrm{c} \frac{\mathrm{i}}{4\pi} U'_\mathrm{c}(b^+_{2,2}-b^-_{2,2}) + \tfrac{1}{2}\mathrm{i}U_\mathrm{c}U'_\mathrm{c} \tag{3.70}$$

is the reciprocal of the scaled complex wavenumber in the linear amplitude (2.14) and we have put

$$\frac{1}{\gamma} = -\frac{1}{\pi}\left(b^+_{2,1}-b^-_{2,1} + \frac{\mathrm{i}\pi U'''_\mathrm{c}}{U'^2_\mathrm{c}}\right)\frac{S_1^2 U_\mathrm{c}}{4\alpha^2}. \tag{3.71}$$

Equation (3.69) is the final result. It determines the amplitude of the instability wave. It must be solved to the upstream boundary condition

$$A \to \mathrm{e}^{\bar{\kappa}\bar{x}+\mathrm{i}\phi_0} \quad \text{as} \quad \bar{x}\to-\infty, \tag{3.72}$$

where the real constant ϕ_0 is an as yet unspecified initial phase factor which was introduced via the arbitrary origin shifts x_0 and X_0 in (3.25) and (3.27).

4. Asymptotic solution of the amplitude equation

The principal result of this paper is given by (3.69) together with the upstream boundary condition (3.72). The numerical solution to this problem, which is discussed in the next section, appears to develop a singularity at a finite value of $\bar{x}$, say $\bar{x}_s$. In this section we determine the asymptotic form of the solution as $\bar{x} \to \bar{x}_s$. To this end we substitute

$$A = \frac{a}{(\bar{x}_s - \bar{x})^{3+i\sigma}}, \tag{4.1}$$

where $\bar{x}_s$ and σ are real constants and a is a complex constant, into the integral of (3.69) and change the integration variables from $\tilde{x}_1$ and $\tilde{x}$ to $(\bar{x}_s - \tilde{x}_1)/(\bar{x}_s - \bar{x})$ and $(\bar{x}_s - \tilde{x})/(\bar{x}_s - \bar{x})$ to show that

$$\int_{-\infty}^{\bar{x}} \int_{-\infty}^{\tilde{x}} K(\bar{x} \mid \tilde{x}, \tilde{x}_1) A(\tilde{x}) A(\tilde{x}_1) A^*(\tilde{x} + \tilde{x}_1 - \bar{x}) \, \mathrm{d}\bar{x}_1 \, \mathrm{d}\tilde{x} = \frac{a|a|^2}{(\bar{x}_s - \bar{x})^{4+i\sigma}} D(\sigma), \tag{4.2}$$

where

$$\begin{aligned} D(\sigma) &= \int_1^\infty \frac{1}{v^{3+i\sigma}} \int_v^\infty \frac{\mathrm{d}u \, \mathrm{d}v}{u^{3+i\sigma}(u+v-1)^{3-i\sigma}} [\![-\tfrac{1}{2}(v-1)^3 \\ &\quad + (v-1)^2 \{u - v - \sin^2\theta [u - v + 4(u-1)\sin^2\theta]\} \\ &\quad + 2(v-1)(u-v)^2 \sin^2\theta (1 - 2\sin^2\theta)]\!] \\ &= \int_1^\infty \frac{1}{v^{3+i\sigma}(v-1)^2} \left\{ \sum_{m=-2}^{2} \frac{\hat{C}_m(v \mid \theta)}{m + i\sigma} \left[\left(\frac{2v-1}{v} \right)^{m+i\sigma} - 1 \right] \right\} \mathrm{d}v \\ &= \int_0^1 \frac{(1-x)^{3+i\sigma}}{x^2} \left\{ \sum_{m=-2}^{2} \frac{\tilde{C}_m(x \mid \theta)}{m + i\sigma} \left[\left(\frac{2v-1}{v} \right)^{m+i\sigma} - 1 \right] \right\} \mathrm{d}x, \end{aligned} \tag{4.3}$$

and the $\hat{C}_m$ and $\tilde{C}_m$ are complicated functions of the indicated arguments which are listed in the Appendix. It is worth noting that $\hat{C}_m$ is a polynomial in $\sin\theta$ whereas $\tilde{C}_m$ is a Fourier series in θ. Carrying out the last integration gives

$$\begin{aligned} D(\sigma) = \sum_{n=1}^{\infty} (-1)^n \Bigg[& \frac{C_{1,0}(n \mid \sigma) + C_{1,2}(n \mid \sigma)\cos 2\theta + C_{1,4}(n \mid \sigma)\cos 4\theta}{n(n+1)(n+2)(n+3)(4+i\sigma)_n} \\ & + \frac{C_{2,0}(n \mid \sigma) + C_{2,2}(n \mid \sigma)\cos 2\theta + C_{2,4}(n \mid \sigma)\cos 4\theta}{(n+1)(n+2)(n+3)(4+i\sigma)_n} \\ & + \frac{C_{3,0}(n \mid \sigma) + C_{3,2}(n \mid \sigma)\cos 2\theta + C_{3,4}(n \mid \sigma)\cos 4\theta}{(n+2)(n+3)(4+i\sigma)_n} \Bigg], \end{aligned} \tag{4.4}$$

where $(\alpha)_n$ denotes the generalized factorial function $\Gamma(\alpha+n)/\Gamma(\alpha)$, and the coefficients $C_{1,0}, \ldots, C_{3,4}$ are given in the Appendix.

$A_{\bar{x}}$ becomes large compared with A as $\bar{x} \to \bar{x}_s$, and the left-hand side of (3.69) is balanced by the integral term on the right-hand side. Substituting (4.1) into the left-hand side shows that the two terms will balance when σ satisfies

$$\frac{D(\sigma)}{(3+i\sigma)} \tan^2\theta = \frac{1}{\gamma\bar{\kappa}|a|^2}. \tag{4.5}$$

Figures 1 and 2 show σ and $|a(\gamma\bar{\kappa})^{\frac{1}{2}}|$ respectively as functions of $\mathrm{Arg}\,(1/\gamma\bar{\kappa})$, which are used to evaluate asymptotic curves in figures 6–11 (shown as dotted lines).

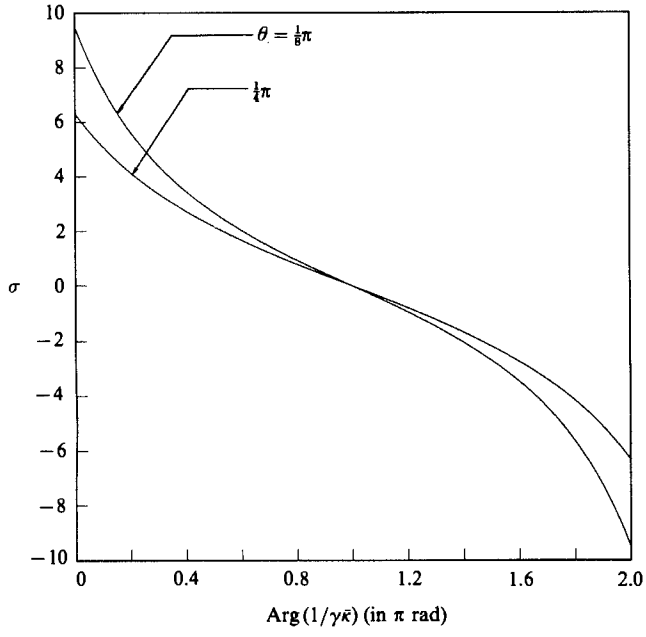

FIGURE 1. Asymptotic exponent σ *vs.* Arg $(1/\gamma\bar{\kappa})$ in π radians.

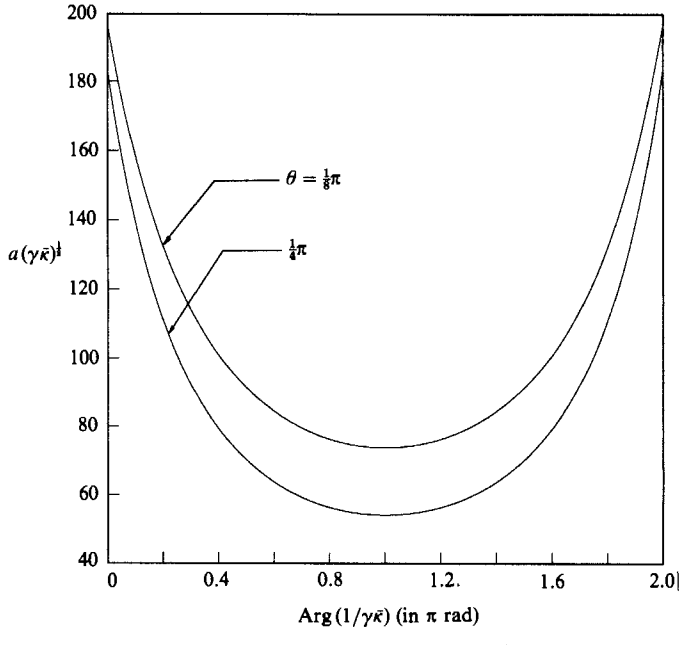

FIGURE 2. Normalized asymptotic amplitude $a(\gamma\bar{\kappa})^{\frac{1}{8}}$ *vs.* Arg $(1/\gamma\bar{\kappa})$ in π radians.

Parts of the derivations in this section were done with MACSYMA (412.61 for DEC VAX 8600 Series) batch programs. Interested readers can contact the second author for the programs.

5. Numerical results and discussion

The relevant solutions to (3.69) and (3.72) involve the two complex parameters $\bar{\kappa}$ and γ, the propagation angle θ, and the still unspecified initial phase factor ϕ_0. But introducing the rescaled variables $A/|\gamma|^{\frac{1}{3}}|\bar{\kappa}|^2$ and $|\bar{\kappa}|\,\bar{x}-\bar{x}_0$, where $\bar{x}_0$ and ϕ_0 are chosen so that

$$\frac{\bar{\kappa}}{|\bar{\kappa}|}\bar{x}_0+\mathrm{i}\phi_0 = \ln|\gamma|^{\frac{1}{3}}|\bar{\kappa}|^2, \tag{5.1}$$

shows that these solutions can be completely characterized by the two imaginary parameters $\ln(\bar{\kappa}/|\bar{\kappa}|)$ and $\ln(\gamma/|\gamma|)$, or equivalently by the arguments of $\bar{\kappa}$ and γ. The real part of $\bar{\kappa}$ is the scaled growth rate of the upstream linear instability wave in the vicinity of its neutral stability point, and the imaginary part is the scaled deviation of the wavenumber from its neutral value corresponding to the prescribed Strouhal number deviation S_1.

Equation (3.69) was solved numerically by using a fourth-order predictor–corrector scheme to advance the solution downstream from the prescribed upstream linear state (equation (3.72)). The double integrals were computed by using the Trapezoidal rule with the upstream 'tails' evaluated analytically from the upstream linear solutions. $\bar{\kappa}$ and γ must, in general, be found numerically by solving the homogeneous and inhomogeneous Rayleigh's equations (2.19) and (2.27). Analytic solutions can be obtained only for the 'tanh' shear layer (Huerre 1980, 1987) where

$$U_c = \frac{U^{(1)}+U^{(2)}}{2\Delta}, U_c' = \bar{\alpha} = 1, \quad U_c''' = -2, \quad b_{2,1}^{+}-b_{2,1}^{-} = 0, \quad b_{2,2}^{+}-b_{2,2}^{-} = 1.$$

Figure 3–5 are plots of the instability wave growth rate $|A|_{\bar{x}}/|A|$ for various values $\arg\gamma$, $\arg\bar{\kappa}$, and $\cos\theta$. We only show results for $-\frac{1}{2}\pi < \arg\bar{\kappa} < 0$ because (3.69) implies that $A(\bar{x},\bar{\kappa}^*,\gamma^*) = A^*(\bar{x},\bar{\kappa},\gamma)$. Notice that the upstream linear growth rate is initially reduced when $\arg(\bar{\kappa}\gamma)$ and θ are both in the ranges $-\frac{1}{2}\pi < \arg\gamma\bar{\kappa} < \frac{1}{2}\pi$ and $-1.583\pi < \theta < 1.583\pi$ (or both outside these ranges). This is because the nonlinear term behaves like $-\gamma C_0|A|^2A$ for small $|A|$, where C_0 is a real function of θ. The effective growth rate is therefore reduced by the factor $1-C_0|A|^2\,\mathrm{Re}(\bar{\kappa}\gamma)/\mathrm{Re}\,\bar{\kappa}$, but (except in the special case $\arg\gamma = \arg\bar{\kappa} = 0$) this trend is eventually reversed, and the growth rate rapidly increases until the amplitude becomes singular at some finite downstream distance for all values of $\bar{\kappa}$ and γ – suggesting an explosive growth of the instability wave there.

This is shown somewhat better in figures 6–8, which are plots of the real part of the scaled instability wave amplitude versus the scaled streamwise coordinate $\bar{x}$. Also shown in the figures are the results computed from the asymptotic solution (4.1), with the singularity location $\bar{x}_s$ determined from the numerical solution. The latter solutions clearly approach the asymptotic result as $|\bar{x}_s-\bar{x}|$ becomes small. Since (4.1) implies that the asymptotic growth rate $|A|_{\bar{x}}/|A|$ behaves like $(|A|/|a|)^{\frac{1}{3}}$ in the vicinity of the singularity, the initial scaling, i.e. growth rate $= O(\epsilon)^{\frac{1}{3}}$, is unchanged by the singularity. This suggests that the basic asymptotic structure of the critical layer will remain intact, and the present solution will not break down until the amplitude $|A|$ of the external instability waves becomes order one. The flow will then be fully nonlinear and unsteady in the main part of the shear layer, i.e. it will be governed by the full Euler's equations there.

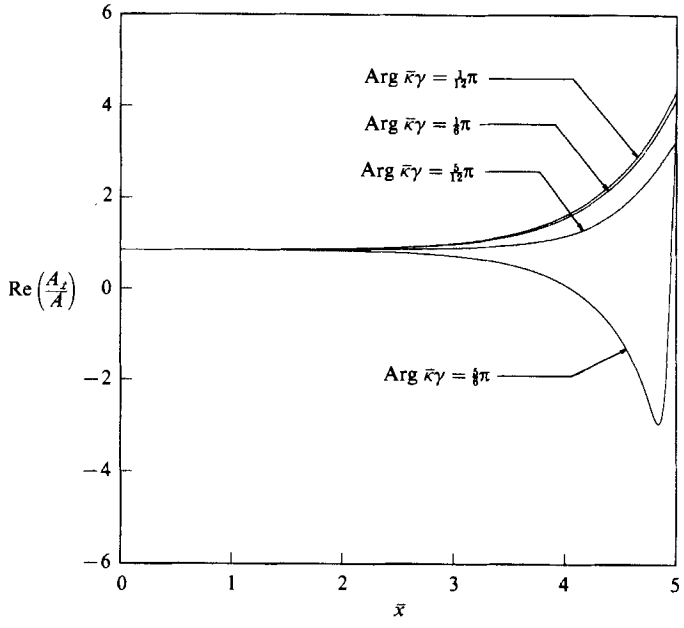

FIGURE 3. Growth rate $\mathrm{Re}\,(A_{\bar{x}}/A)$ *vs.* scaled streamwise coordinate $\bar{x}$ for $\theta = \frac{1}{8}\pi$ and $\mathrm{Arg}\,\bar{\kappa} = -\frac{1}{6}\pi$.

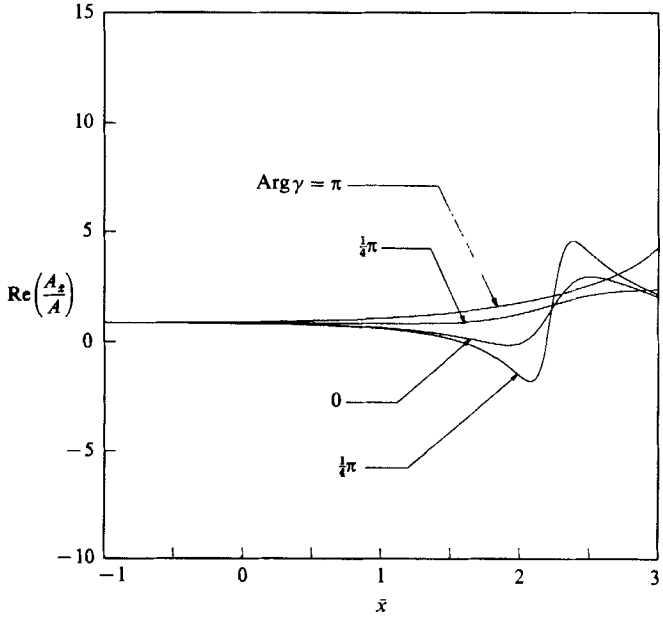

FIGURE 4. Growth rate $\mathrm{Re}\,(A_{\bar{x}}/A)$ *vs.* scaled streamwise coordinate $\bar{x}$ for $\theta = \frac{1}{4}\pi$ and $\mathrm{Arg}\,\bar{\kappa} = -\frac{1}{6}\pi$.

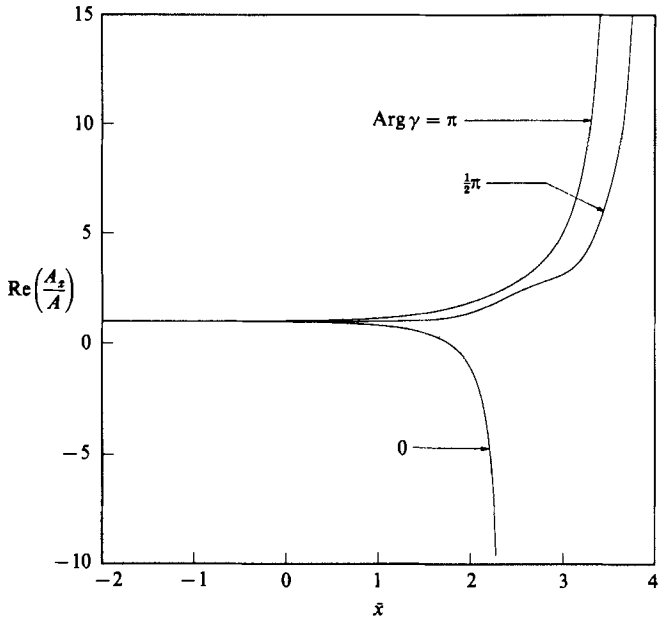

FIGURE 5. Growth rate $\mathrm{Re}\,(A_x/A)$ *vs.* scaled streamwise coordinate $\bar{x}$ for $\theta = \frac{1}{4}\pi$ and $\mathrm{Arg}\,\bar{\kappa} = 0$.

This is quite different from the two-dimensional nonlinear critical behaviour in the analysis of Goldstein & Leib (1988) where the critical-layer nonlinearity produces a redistribution of vorticity that rapidly reduces the instability wave growth rate to zero. Three-dimensional effects allow for vortex stretching in the present analysis, and this completely counteracts the growth reduction effect to produce the explosive instability wave growth. This phemomenon is probably masked at subsonic speeds by the fact that the linear growth rate of the three-dimensional wave is much smaller than that of the two-dimensional wave. The latter wave can alter the critical-layer structure of the oblique waves, and the present analysis assumes that the two-dimensional wave is completely absent in the nonlinear region. It should be possible to eliminate the two-dimensional wave in carefully controlled subsonic experiments, but it would probably be much easier to observe the phenomenon at supersonic speeds where the most rapidly growing linear mode is oblique. While the basic amplitude equation (3.69) was derived only for incompressible flow, it applies to the compressible case as well, and there is no *a priori* restriction on the Mach number. It is worth noting that the nonlinear critical-layer effects should be much more important at higher Mach numbers, because the linear growth rate rapidly decreases with increasing Mach number (Jackson & Grosch 1988).

Figures 6–8 show that the instability wave amplitude undergoes successive oscillation upstream of the singularity. Similar behaviour was observed in the two-dimensional analysis of Goldstein & Leib (1988) and in the calculations of Benney & Maslowe (1975), Huerre (1977), and Miura & Sato (1978). The amplitude oscillations imply periodic reversal of energy transfer between the fluctuations and the mean flow, and possibly between the fluctuations themselves. By considering the Reynolds-stress changes that occur with nutating elliptic vortices, Browand & Ho (1983) came up with a simple kinematic explanation for this phenomenon. The reader is referred to Ho & Huerre (1984, p. 410) for details.

Viscous effects will undoubtedly alter the critical-layer behaviour described above.

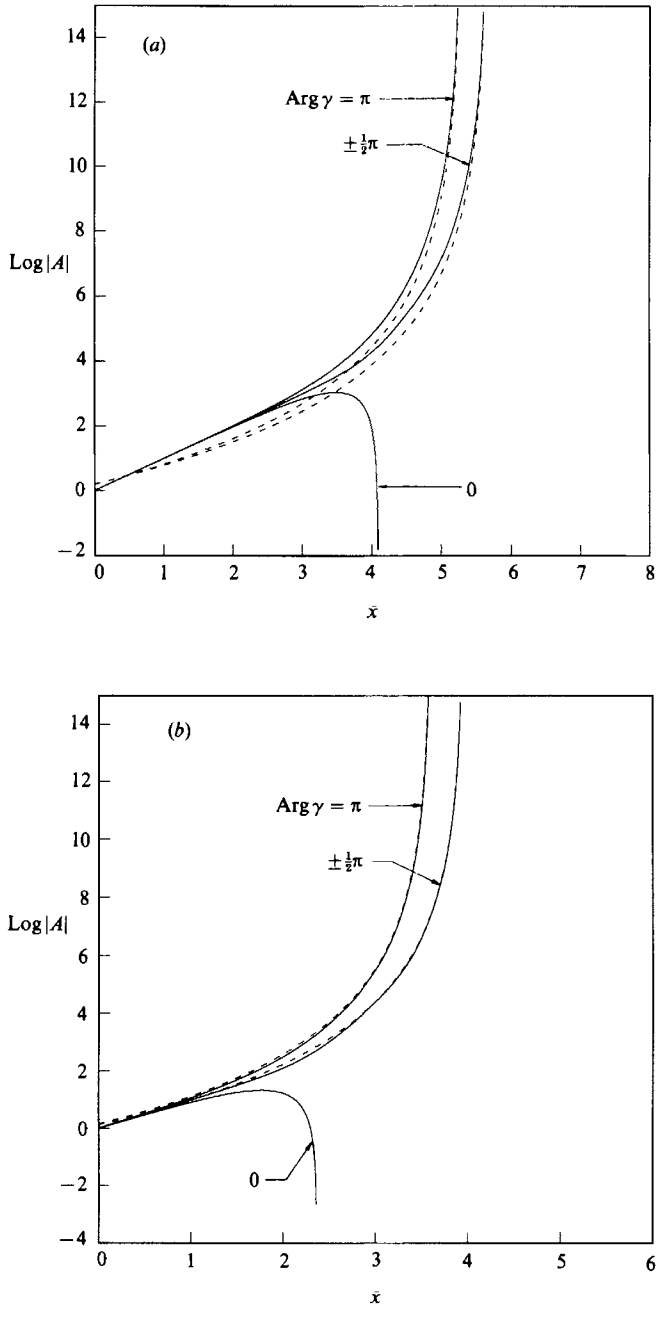

FIGURE 6. Amplitude $\log|A|$ *vs.* scaled streamwise coordinate $\bar{x}$ for $\operatorname{Arg}\bar{\kappa} = 0$, and (*a*) $\theta = \frac{1}{8}\pi$, (*b*) $\theta = \frac{1}{4}\pi$.

We decided not to include them because they would greatly complicate an already complex analysis. They were, however, included in the simpler analysis of Goldstein & Leib (1989), and we expect them to act similarly in the present situation. The former analysis suggests that viscous effects always delay the explosive growth and that they will eliminate it entirely for a certain range of values of $\gamma, \bar{\kappa}$, and θ,

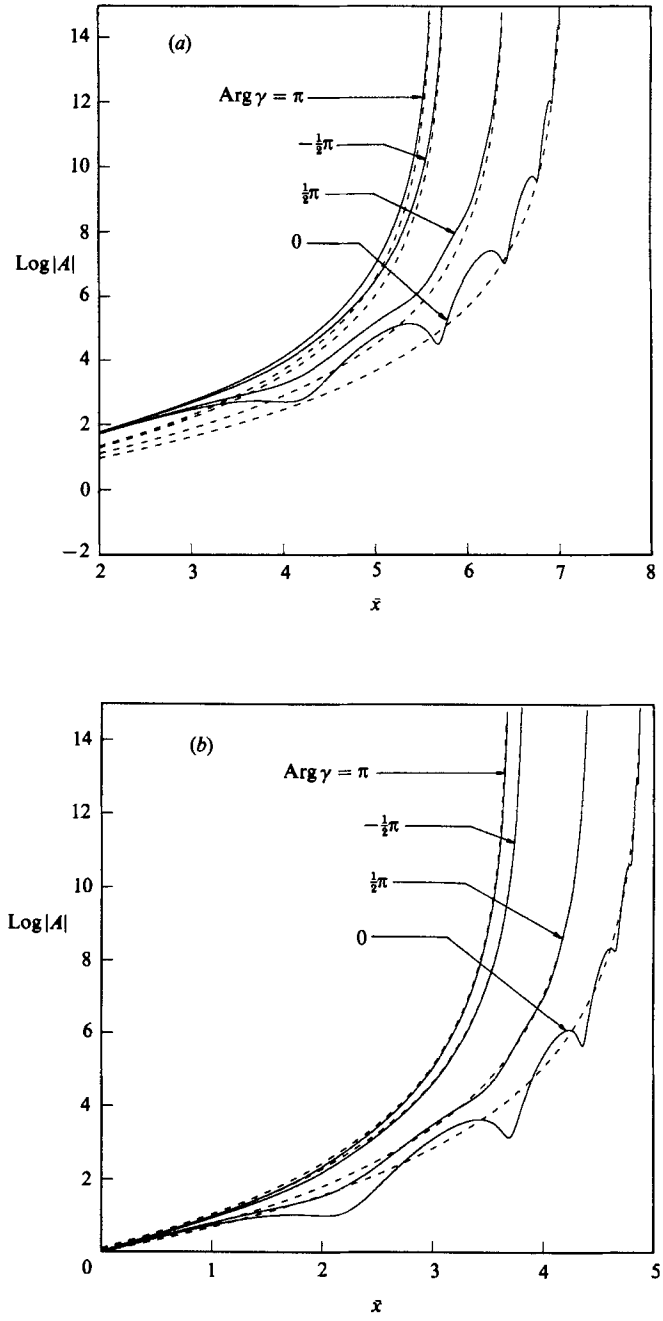

FIGURE 7. Amplitude log $|A|$ *vs.* scaled streamwise coordinate $\bar{x}$ for $\operatorname{Arg}\bar{\kappa} = -\frac{1}{8}\pi$, and (*a*) $\theta = \frac{1}{8}\pi$, (*b*) $\theta = \frac{1}{4}\pi$.

provided an appropriate scaled viscous parameter exceeds a certain finite value. In that case, the solution will just go to a finite-amplitude equilibrium state further downstream.

While the present scaling may seem to be rather special, the composite expansion technique of Goldstein & Leib (1988) shows that the instability wave adjusts to the

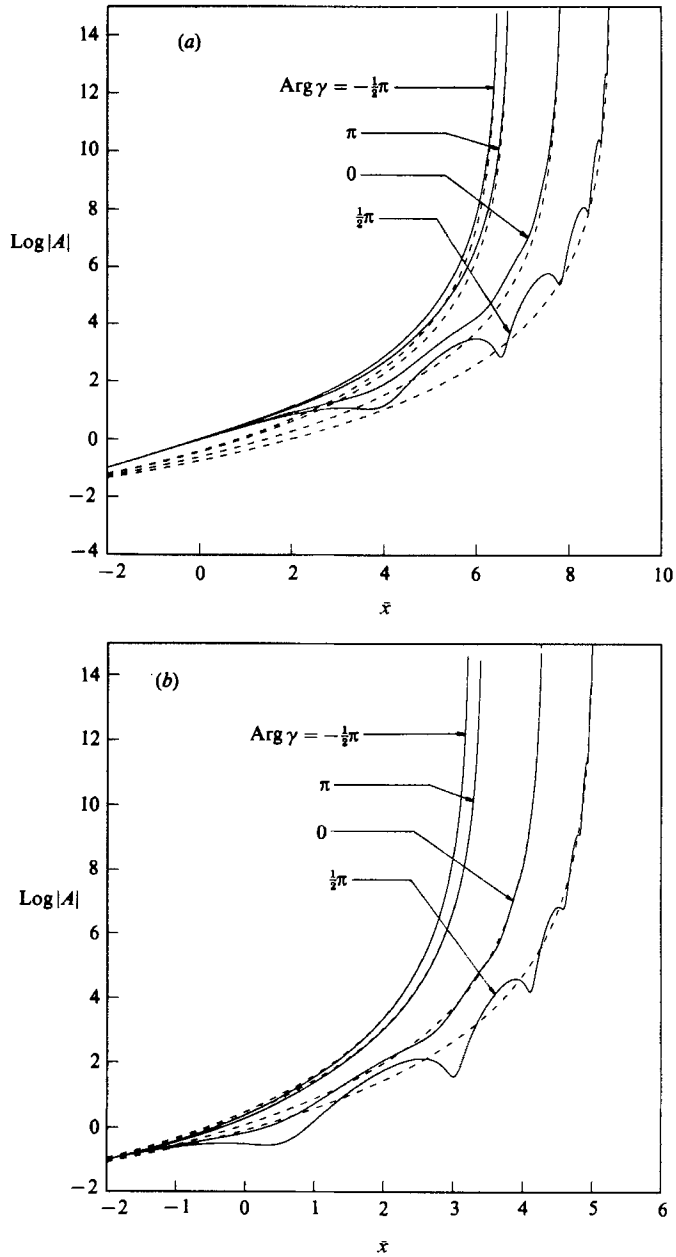

FIGURE 8. Amplitude log $|A|$ *vs.* scaled streamwise coordinate $\bar{x}$ for Arg $\bar{\kappa} = -\frac{1}{3}\pi$, and (*a*) $\theta = \frac{1}{8}\pi$, (*b*) $\theta = \frac{1}{4}\pi$.

proper scaling automatically as it propagates downstream toward the neutral stability point.† The nonlinear region actually sets its own location in the final composite expansion. The only requirement is that the instability wave amplitude remains fairly small in the region where the linear growth is fairly small. This

† As in Goldstein & Leib (1988), the nonlinear solution can be considered to be an inner solution in a composite expansion whose outer solution is the linear wave corrected for non-parallel mean flow effects.

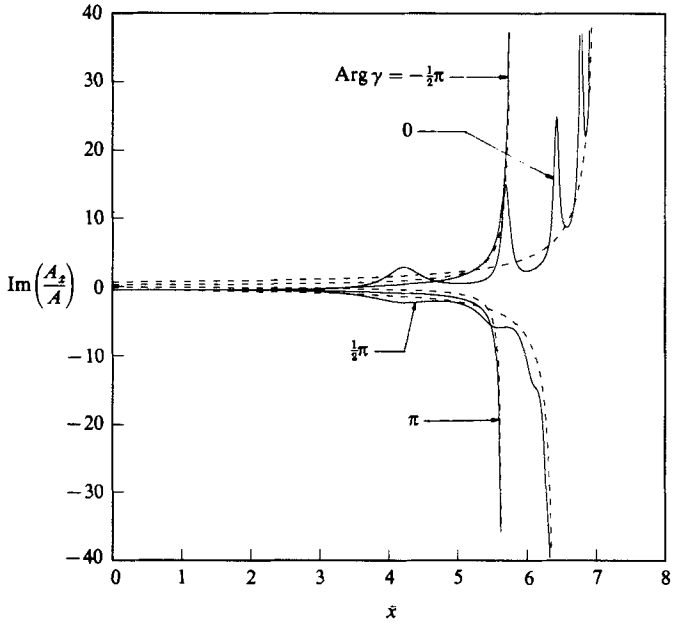

FIGURE 9. Phase Im $(A_{\bar{x}}/A)$ *vs.* scaled streamwise coordinate $\bar{x}$ for $\theta = \frac{1}{8}\pi$ and Arg $\bar{\kappa} = -\frac{1}{6}\pi$.

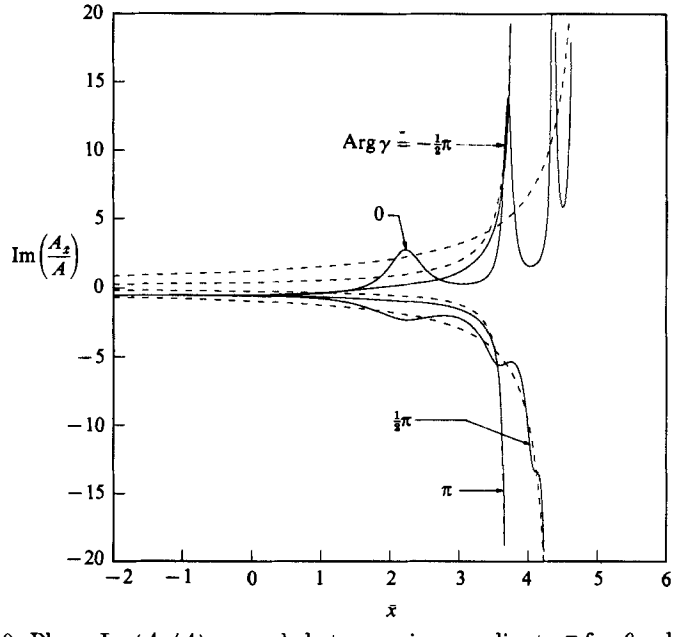

FIGURE 10. Phase Im $(A_{\bar{x}}/A)$ *vs.* scaled streamwise coordinate $\bar{x}$ for $\theta = \frac{1}{4}\pi$ and Arg $\bar{\kappa} = -\frac{1}{6}\pi$.

requirement should be very non-restrictive at supersonic speeds where the linear growth rate is always small. However, the experiments show that nonlinearity sets in at very small amplitudes, even at subsonic speeds, which suggests that the nonlinear effects are localized spatially and therefore confined to the critical layer (since this is the region where nonlinearity would first come into play; Goldstein & Leib 1988; Goldstein & Hultgren 1988).

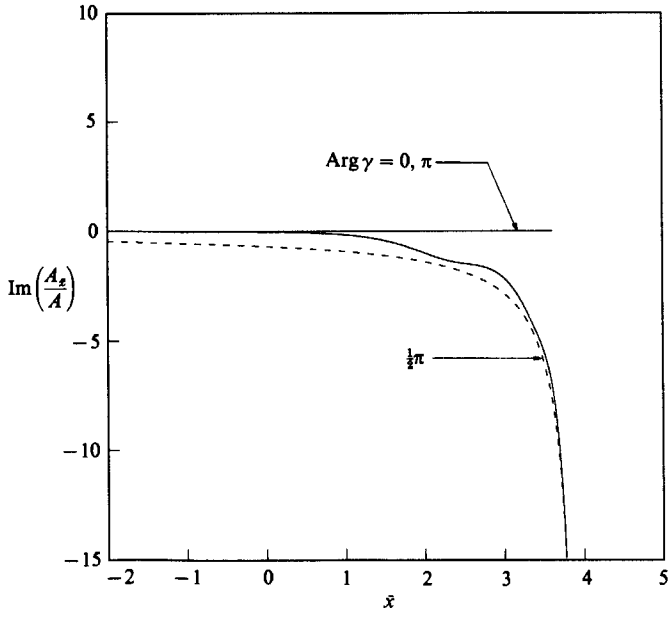

FIGURE 11. Phase $\mathrm{Im}\,(A_x/A)$ *vs.* scaled streamwise coordinate $\bar{x}$ for $\theta = \frac{1}{4}\pi$ and $\mathrm{Arg}\,\bar{\kappa} = 0$.

Equations (2.7), (3.25), and (4.1) show that the explosive growth occurs when

$$x - x_s = O(1),$$

where

$$x_s \equiv \frac{\bar{x}_s + \bar{x}_0}{-\frac{1}{2}\epsilon^{\frac{1}{3}} S_1 U_c'}$$

is the singularity location in the unscaled streamwise coordinates. The streamwise extent of the fully nonlinear region is therefore of the same order as the shear-layer width.

It is also worth noting that the asymptotic instability wave amplitude is uniquely determined by the asymptotic solution and is therefore independent of the upstream conditions. Figures 9–11 show the wavelength reduction $\mathrm{Im}\,(A_x/A)$ as a function of the scaled coordinate $\bar{x}$. The asymptotic results computed from (4.1) are indicated by the dashed lines.

The authors would like to thank Dr Lennart Hultgren for his helpful comments on the manuscript and Dr S. J. Leib for helping with the computer program.

Appendix

The detailed expressions for coefficients used in (4.3) and (4.4) are

$$\hat{C}_2 = \frac{3v-1}{2(v-1)} - \frac{v(3v-1)}{(v-1)^2}\sin^2\theta + 4\frac{v^2-v+1}{(v-1)^2}\sin^4\theta, \tag{A 1}$$

$$\hat{C}_1 = -\frac{7v-3}{v-1} + \frac{17v^2-10v+1}{(v-1)^2}\sin^2\theta - 4\frac{5v^2-4v+3}{(v-1)^2}\sin^4\theta, \tag{A 2}$$

$$\hat{C}_0 = 6\frac{2v-1}{v-1} - \frac{35v^2-28v+5}{(v-1)^2}\sin^2\theta + 8\frac{5v^2-4v+2}{(v-1)^2}\sin^4\theta, \tag{A 3}$$

$$\hat{C}_{-1} = -\frac{9v-5}{v-1} + \frac{31v^2-30v+7}{(v-1)^2}\sin^2\theta - 4\frac{9v^2-8v+3}{(v-1)^2}\sin^4\theta, \tag{A 4}$$

$$\hat{C}_{-2} = \frac{5v-3}{2(v-1)} - \frac{10v^2-11v+3}{(v-1)^2}\sin^2\theta + 4\frac{3v^2-3v+1}{(v-1)^2}\sin^4\theta, \tag{A 5}$$

$$\tilde{C}_2 = \tfrac{1}{2}(1-2x+4x^2) - \tfrac{1}{2}(2-5x+4x^2)\cos 2\theta + \tfrac{1}{2}(1-x+x^2)\cos 4\theta, \tag{A 6}$$

$$\tilde{C}_1 = -(2-3x+7x^2) + \tfrac{1}{2}(8-16x+11x^2)\cos 2\theta - \tfrac{1}{2}(4-2x+3x^2)\cos 4\theta, \tag{A 7}$$

$$\tilde{C}_0 = \tfrac{1}{2}(6-6x+19x^2) - \tfrac{1}{2}(12-18x+11x^2)\cos 2\theta + (3+2x^2)\cos 4\theta, \tag{A 8}$$

$$\tilde{C}_{-1} = -(2-x+6x^2) + \tfrac{1}{2}(8-8x+5x^2)\cos 2\theta - \tfrac{1}{2}(4+2x+3x^2)\cos 4\theta, \tag{A 9}$$

$$\tilde{C}_{-2} = \tfrac{1}{2}(1+3x^2) - \tfrac{1}{2}(2-x+x^2)\cos 2\theta + \tfrac{1}{2}(1+x+x^2)\cos 4\theta, \tag{A 10}$$

$$C_{1,0} = \tfrac{1}{2}(-1-\mathrm{i}\sigma)_{n+2} - 2(-\iota\sigma)_{n+2} + 3(1-\mathrm{i}\sigma)_{n+2} - 2(2-\mathrm{i}\sigma)_{n+2} + \tfrac{1}{2}(3-\mathrm{i}\sigma)_{n+2}, \tag{A 11}$$

$$C_{2,0} = -(-1-\mathrm{i}\sigma)_{n+2} + 3(-\mathrm{i}\sigma)_{n+2} - 3(1-\mathrm{i}\sigma)_{n+2} + (2-\mathrm{i}\sigma)_{n+2}, \tag{A 12}$$

$$C_{3,0} = 2(-1-\mathrm{i}\sigma)_{n+2} - 7(-\mathrm{i}\sigma)_{n+2} + \tfrac{19}{2}(1-\mathrm{i}\sigma)_{n+2} - 6(2-\mathrm{i}\sigma)_{n+2} + \tfrac{3}{2}(3-\mathrm{i}\sigma)_{n+2}, \tag{A 13}$$

$$C_{1,2} = -(-1-\mathrm{i}\sigma)_{n+2} + 4(-\mathrm{i}\sigma)_{n+2} - 6(1-\mathrm{i}\sigma)_{n+2} + 4(2-\mathrm{i}\sigma)_{n+2} - (3-\mathrm{i}\sigma)_{n+2}, \tag{A 14}$$

$$C_{2,2} = \tfrac{5}{2}(-1-\mathrm{i}\sigma)_{n+2} - 8(-\mathrm{i}\sigma)_{n+2} + 9(1-\mathrm{i}\sigma)_{n+2} - 4(2-\mathrm{i}\sigma)_{n+2} + \tfrac{1}{2}(3-\mathrm{i}\sigma)_{n+2}, \tag{A 15}$$

$$C_{3,2} = -2(-1-\mathrm{i}\sigma)_{n+2} + \tfrac{11}{2}(-\mathrm{i}\sigma)_{n+2} - \tfrac{11}{2}(1-\mathrm{i}\sigma)_{n+2} + \tfrac{5}{2}(2-\mathrm{i}\sigma)_{n+2} - \tfrac{1}{2}(3-\mathrm{i}\sigma)_{n+2}, \tag{A 16}$$

$$C_{1,4} = \tfrac{1}{2}(-1-\mathrm{i}\sigma)_{n+2} - 2(-\mathrm{i}\sigma)_{n+2} + 3(1-\mathrm{i}\sigma)_{n+2} - 2(2-\mathrm{i}\sigma)_{n+2} + \tfrac{1}{2}(3-\mathrm{i}\sigma)_{n+2}, \tag{A 17}$$

$$C_{2,4} = -\tfrac{1}{2}(-1-\mathrm{i}\sigma)_{n+2} + (-\mathrm{i}\sigma)_{n+2} - (2-\mathrm{i}\sigma)_{n+2} + \tfrac{1}{2}(3-\mathrm{i}\sigma)_{n+2}, \tag{A 18}$$

$$C_{3,4} = \tfrac{1}{2}(-1-\mathrm{i}\sigma)_{n+2} - \tfrac{3}{2}(-\mathrm{i}\sigma)_{n+2} + 2(1-\mathrm{i}\sigma)_{n+2} - \tfrac{3}{2}(2-\mathrm{i}\sigma)_{n+2} + \tfrac{1}{2}(3-\mathrm{i}\sigma)_{n+2}. \tag{A 19}$$

REFERENCES

BENNEY, D. J. & MASLOWE, S. A. 1975 The evolution in space and time of nonlinear waves in parallel shear flows. *Stud. Appl. Maths* **54**, 181–205.

BROWAND, F. K. & HO, C. M. 1983 The mixing layer: an example of quasi two-dimensional turbulence. *J. Méc. Theor. Appl.* **2**, 99–120.

GOLDSTEIN, M. E. & HULTGREN, L. S. 1988 Nonlinear spatial evolution of an externally excited instability wave in a free shear layer. *J. Fluid Mech.* **197**, 295–330.

GOLDSTEIN, M. E. & LEIB, S. J. 1988 Nonlinear roll-up of externally excited free shear layers. *J. Fluid Mech.* **191**, 481–515.

GOLDSTEIN, M. E. & LEIB, S. J. 1989 Nonlinear evolution of oblique waves on compressible shear layers. *J. Fluid Mech.* **207**, 73–96.

GROPENGEISSER, H. 1969 Study of the stability of boundary layers and compressible fluids. *Deutsche Luft- und Raunfahnt, Rep.* DLR-FB-69-25. (NASA translations TTF-12, 786.)

HICKERNELL, F. J. 1984 Time-dependent critical layers in shear flows on the beta-plane. *J. Fluid Mech.* **142**, 431–449.

HO, C. M. & HUERRE, P. 1984 Perturbed free shear layers. *Ann. Rev. Fluid Mech.* **16**, 365–424.

HUERRE, P. 1977 Nonlinear instability of free shear layers. In *Laminar–Turbulent Transition, AGARD CP*, pp. 224–229.

HUERRE, P. 1980 The nonlinear stability of a free shear layer in the viscous critical layer regime. *Phil. Trans. R. Soc. Lond.* A **293**, 643–672.

HUERRE, P. 1987 On the Landau constant in mixing layers. *Proc. R. Soc. Lond.* A **409**, 369–381.

HUERRE, P. & SCOTT, J. F. 1980 Effects of critical layer structure on the nonlinear evolution of waves in free shear layers. *Proc. R. Soc. Lond.* A **371**, 500–524.

JACKSON, T. L. & GROSCH, C. E. 1988 Spatial stability of a compressible mixing layer. *NASA CR*-181671.

MASLOWE, S. 1986 Critical layers in shear flows. *Ann. Rev. Fluid. Mech.* **18**, 405–432.

MIURA, A. & SATO, T. 1978 Theory of vortex nutation and amplitude oscillation in an inviscid shear instability. *J. Fluid Mech* **86**, 33–47.

ROBINSON, J. L. 1974 The inviscid nonlinear instability of parallel shear flows. *J. Fluid Mech.* **63**, 723–752.

STEWARTSON, K. 1981 Marginally stable inviscid flows with critical layer. *IMA J. Appl. Maths* **27**, 133–175.